J|A|C|S
ARTICLES
Published on Web 11/26/2002

Thermal and Photochemical Rearrangement of Bicyclo[3.1.0]hex-3-en-2-one to the Ketonic Tautomer of Phenol. Computational Evidence for the Formation of a Diradical Rather than a Zwitterionic Intermediate

Isabel Gómez,[†] Santiago Olivella,*[,‡] Mar Reguero,*[,†] Antoni Riera,[§] and Albert Solé[⊥]

Contribution from the Departament de Química Física i Inorgànica i Institut d'Estudis Avançats, Universitat Rovira i Virgili, Pl. Tarraco 1, 43005 Tarragona, Catalonia, Spain, Institut d'Investigacions Químiques i Ambientals de Barcelona, CSIC, Jordi Girona 18, 08034-Barcelona, Catalonia, Spain, Parc Científic de Barcelona i Departament de Química Orgànica, Universitat de Barcelona, Martí i Franquès 1, 08028-Barcelona, Catalonia, Spain, and Centre Especial de Recerca en Química Teòrica i Departament de Química Física, Universitat de Barcelona, Martí i Franquès 1, 08028-Barcelona, Catalonia, Spain

Received March 27, 2002. Revised Manuscript Received July 1, 2002

Abstract: The ground state (S_0) and lowest-energy triplet state (T_1) potential energy surfaces (PESs) concerning the thermal and photochemical rearrangement of bicyclo[3.1.0]hex-3-en-2-one (**8**) to the ketonic tautomer of phenol (**11**) have been extensively explored using ab initio CASSCF and CASPT2 calculations with several basis sets. State T_1 is predicted to be a triplet $\pi\pi^*$ lying 66.5 kcal/mol above the energy of the S_0 state. On the S_0 PES, the rearrangement of **8** to **11** is predicted to occur via a two-step mechanism where the internal cyclopropane C−C bond is broken first through a high energy transition structure (**TS1-S_0**), leading to a singlet intermediate (**10-S_0**) lying 25.0 kcal/mol above the ground state of **8**. Subsequently, this intermediate undergoes a 1,2-hydrogen shift to yield **11** by surmounting an energy barrier of only 2.7 kcal/mol at 0 K. The rate-determining step of the global rearrangement is the opening of the three-membered ring in **8**, which involves an energy barrier of 41.2 kcal/mol at 0 K. This high energy barrier is consistent with the fact that the thermal rearrangement of umbellulone to thymol is carried out by heating at 280 °C. Regarding the photochemical rearangement, our results suggest that the most efficient route from the T_1 state of **8** to ground state **11** is the essentially barrierless cleavage of the internal cyclopropane C−C bond followed by radiationless decay to the S_0 state PES via intersystem crossing (ISC) at a crossing point (**S_0/T_1-1**) located at almost the same geometry as **TS1-S_0**, leading to the formation of **10-S_0** and the subsequent low-barrier 1,2-hydrogen shift. The computed small spin−orbit coupling between the T_1 and S_0 PESs at **S_0/T_1-1** (1.2 cm^{-1}) suggests that the ISC between these PESs is the rate-determining step of the photochemical rearrangement **8** → **11**. Finally, computational evidence indicates that singlet intermediate **10-S_0** should not be drawn as a zwitterion, but rather as a diradical having a polarized C═O bond.

Introduction

Umbellulone (**1**) is a monoterpene ubiquitously found in the essential oils of plants.[1,2] In 1958, Wheeler and Eastman[3] observed that samples of **1** that had been exposed to sunlight invariably contained thymol (**2**). This observation prompted him to study the pyrolysis and photolysis of umbellulone. Irradiation of neat **1** for 4 h by a H400 mercury arc lamp gave **2** in nearly quantitative yield, whereas heating at 280 °C afforded a mixture of **2** and sym-thymol (**3**) (Scheme 1). Wheeler and Eastman suggested the possibility of a free radical pathway for the photochemical reaction and an ionic mechanism for the thermal rearrangement. Some years later, Chapman and co-workers[4] studied the photochemical reaction at low temperature. Monitoring by IR the irradiation of **1** in liquid nitrogen, they could identify dienone **4**, the ketonic tautomer of **2**, as an intermediate (Scheme 1). They also detected and trapped a ketene intermediate working at −190°, although it was not clear that it was involved in the reaction at higher temperatures.

* To whom correspondence should be addressed. E-mail: sonqtc@cid.csic.es.
[†] Universitat Rovira i Virgili.
[‡] Institut d'Investigacions Químiques i Ambientals de Barcelona, CSIC.
[§] Parc Científic de Barcelona i Departament de Química Orgànica, Universitat de Barcelona.
[⊥] Centre Especial de Recerca en Química Teòrica i Departament de Química Física, Universitat de Barcelona.

(1) (a) Gillam, A. E.; West, T. F. *J. Chem. Soc.* **1945**, 95−98. (b) Wheeler, J. W.; Chung, R. H. *J. Org. Chem.* **1969**, *34*, 1149−1151.
(2) (a) Malizia, R. A.; Cardell, D. A.; Molli, J. S.; Gonzalez, S.; Guerra, P. E.; Grau, R. J. *J. Essent. Oil Res.* **2000**, *12*, 59−63. (b) Chanegriha, N.; Baaliouamer, A.; Meklati, B.-Y.; Chretien, J. R.; Keravis, G. *J. Essent. Oil Res.* **1997**, *9*, 555−559. (c) Schearer, W. R. *J. Nat. Prod.* **1984**, *47*, 964−9. (d) Satar, S. *Pharmazie* **1984**, *39*, 66−7. (e) Buttery, R. G.; Kamm, J. A. *J. Agric. Food Chem.* **1980**, *28*, 978−81.
(3) Wheeler, J. W.; Eastman, R. H. *J. Am. Chem. Soc.* **1959**, *81*, 236−237.
(4) Barber, L.; Chapman, O. L.; Lassila, J. D. J. *Am. Chem. Soc.* **1968**, *90*, 5933−5934.

Scheme 1

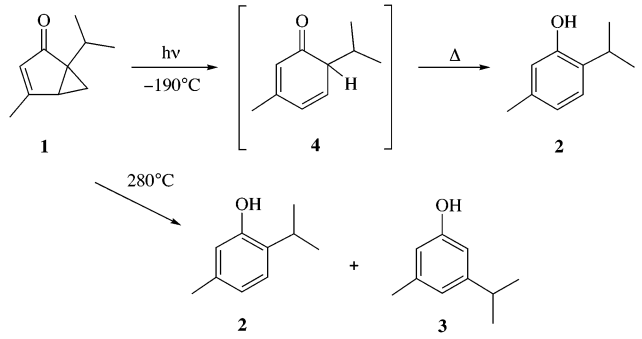

Scheme 2

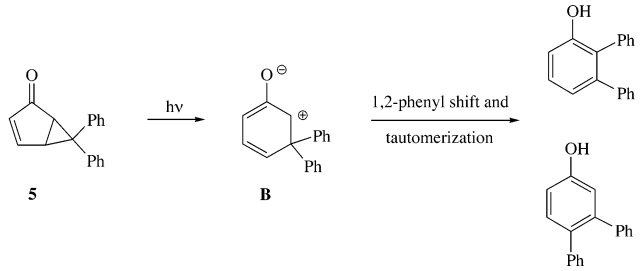

Somewhat surprisingly, to the best of our knowledge, there are no more mechanistic studies on this interesting transformation. Similar photochemical rearrangements in other bicyclo[3.1.0]hex-3-en-2-ones have been described,[5] although the number of studies is scarce as compared to the large number of references on the photochemical preparation of these bicyclic compounds from cyclohexenones,[6] phenols,[7] and cyclohexadienones.[8,9]

In 1961, Zimmerman and Schuster[8a] suggested that the photochemical transformation of 6,6-diphenylbicyclo[3.1.0]hex-3-en-2-one (**5**) to yield 2,3- and 3,4-disubstituted phenols proceeds via the so-called zwitterion **B** (Scheme 2). The"existence" of this zwitterionic intermediate was supported by the fact that it could be independently generated without light, affording the same phenolic ratio as photochemically.[10] This and other experimental observations such as nucleophilic trapping[11] conduced to a general acceptance of zwitterion **B** as a true photochemical intermediate. As a consequence, this zwitterion has been postulated in many photochemical processes[12] such as the photochemistry of other bicyclo[3.1.0]hex-3-en-2-ones or cyclohexadienones.[5]

Scheme 3

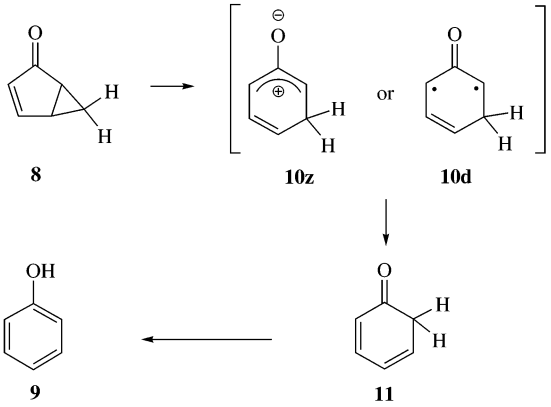

More recently, it has been found that 3-substituted bicyclo[3.1.0]hex-3-en-2-ones (**6**), easily prepared[13] by Pauson−Khand reaction of terminal alkynes with cyclopropene, afforded *ortho*-phenols **7** quantitatively upon sunlight exposure or irradiation at 350 nm.[14] This result prompted the theoretical study[14] of the

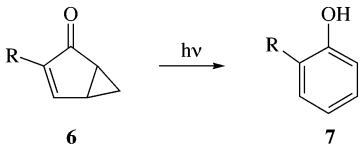

reaction pathway for the prototype rearrangement of bicyclo[3.1.0]hex-3-en-2-one (**8**) to phenol (**9**) using 3 × 3 configuration interaction calculations,[15] at the semiempirical AM1 level.[16] From this study, it was concluded that the photorearrangement of **8** to **9** occurs through a stepwise mechanism involving the cleavage of the internal cyclopropane C−C bond on the potential energy surface of the lowest-energy triplet state, leading to a diradical intermediate **10d** with nearly the same energy for the triplet and singlet states (Scheme 3). This intermediate, already in its ground-state singlet, would undergo a hydrogen migration to hexa-2,4-dienone (**11**) which tautomerizes to **9**.

The impossibility to locate any energy minimum with an electronic structure that could be assigned to the zwitterion intermediate **B** suggested by Zimmermann (e.g., **10z**) was somewhat surprising and revealed the need for a new theoretical study of the photorearrangement of **8** to give **9** based on ab initio calculations at a higher level of theory. In this paper, we report CASSCF and CASPT2 calculations of the pathway **8** → **11** on the lowest-energy singlet and triplet state potential energy surfaces. These calculations support a mechanistic model for

(5) (a) Zimmerman, H. E.; Sebek, P.; Zhu, Z. *J. Am. Chem. Soc.* **1998**, *120*, 8549−8550. (b) Matsuura, T.; Meng, J. B.; Ito, Y.; Irie, M.; Fukuyama, K. *Tetrahedron* **1987**, *43*, 2451−2456. (c) Fisch, M. H.; Richards, J. H. *J. Am. Chem. Soc.* **1968**, *90*, 1547−1553. (d) Dauben, W. G.; Hecht, S. *J. Org. Chem.* **1998**, *63*, 6102−6107.

(6) (a) Zimmerman, H. E.; Zhu, Z. *J. Am. Chem. Soc.* **1995**, *117*, 5245−5262. (b) Schuster, D. I.; Brown, R. H.; Resnick, B. M. *J. Am. Chem. Soc.* **1978**, *100*, 4504−4512. (c) Dauben, W. G.; Spitzer, W. A.; Kellogg, M. S. *J. Am. Chem. Soc.* **1971**, *93*, 3674−3677.

(7) (a) Kakiuchi, K.; Ue, M.; Yamaguchi, B.; Nishimoto, A.; Tobe, Y. *Bull. Chem. Soc. Jpn.* **1991**, *64*, 3468−3470. (b) Baeckström, P.; Jacobsson, U.; Koutek, B.; Norin, T. *J. Org. Chem.* **1985**, *50*, 3728−3732.

(8) (a) Zimmerman, H. E.; Schuster, D. I. *J. Am. Chem. Soc.* **1961**, *83*, 4486−4488. (b) Zimmerman, H. E. *Angew. Chem., Int. Ed. Engl.* **1969**, *8*, 1−11. (c) Schultz, A. G.; Lavieri, F. P.; Macielag, M. *Tetrahedron Lett.* **1986**, *27*, 1481−1484. (d) Schultz, A. G. *Pure Appl. Chem.* **1988**, *60*, 981−988. (e) Zimmerman, H. E.; Lynch, D. C. *J. Am. Chem. Soc.* **1985**, *107*, 7745−7756. (f) Quinkert, G.; Kleiner, E.; Freitag, B. J.; Glenneberg, J.; Billhardt, U. M.; Cech, F.; Schmieder, K. R.; Schudok, C.; Steinmetzer, H. C.; Bats, J. W.; Zimmermann, G.; Dürner, G.; Rehm, D.; Paulus, E. F. *Helv. Chim. Acta* **1986**, *69*, 469−537. (g) Quinkert, G.; Scherer, S.; Reichert, D.; Nestler, H. P.; Wennemers, H.; Ebel, A.; Urbahns, K.; Wagner, K.; Michaelis, K. P.; Wiech, G.; Prescher, G.; Bronstert, B.; Freitag, B. J.; Wicke, I.; Lisch, D.; Belik, P.; Crecelius, T.; Horstermann, D.; Zimmermann, G.; Bats, J. W.; Durner, G.; Rehm, D. *Helv. Chim. Acta* **1997**, *80*, 1683−1772.

(9) Schuster, D. I. *Acc. Chem. Res.* **1978**, *11*, 65−73.

(10) (a) Zimmerman, H. E.; Crumrine, D. S.; Doepp, D.; Huyffer, P. S. *J. Am. Chem. Soc.* **1969**, *91*, 434−45. (b) Zimmerman, H. E.; Epling, G. A. *J. Am. Chem. Soc.* **1972**, *94*, 7806−11. (c) Zimmerman, H. E. *Tetrahedron* **1974**, *30*, 1617−1628.

(11) (a) Patel, D. J.; Schuster, D. I. *J. Am. Chem. Soc.* **1968**, *90*, 5137−5145. (b) Schuster, D. I.; Patel, D. J. *J. Am. Chem. Soc.* **1968**, *90*, 5145−5152. (c) Schuster, D. I.; Liu, K.-C. *Tetrahedron* **1981**, *37*, 3329−3338.

(12) (a) Fisch, M. H. *J. Chem. Soc. D* **1969**, 1472−3. (b) Schultz, A. G.; Reilly, J. *J. Am. Chem. Soc.* **1992**, *114*, 5068−73. (c) Zimmerman, H. E.; Sebek, P. *J. Am. Chem. Soc.* **1997**, *119*, 3677−3690.

(13) Marchueta, I.; Verdaguer, X.; Moyano, A.; Pericàs, M. A.; Riera, A. *Org. Lett.* **2001**, *3*, 3193−3196.

(14) Marchueta, I.; Olivella, S.; Solà, Ll.; Moyano, A.; Pericàs, M. A.; Riera, A. *Org. Lett.* **2001**, *3*, 3197−3200.

(15) Salem, L.; Rowland, C. *Angew. Chem., Int. Ed. Engl.* **1972**, *11*, 92−111.

(16) Dewar, M. J. S.; Zoebisch, E. G.; Healy, E. F.; Stewart, J. J. P. *J. Am. Chem. Soc.* **1985**, *107*, 3902−3909.

the thermal and photochemical rearrangements of substituted bicyclo[3.1.0]hex-3-en-2-ones to phenols.

Theoretical Background and Computational Details

It is usually assumed[5,8,9] that the photochemical rearrangement of substituted bicyclo[3.1.0]hex-3-en-2-ones originates from a short-lived triplet excited state, hereafter designated by T_1, formed after initial photoexcitation of its singlet ground-state, hereafter designated by S_0, to the excited singlet $^1(n\text{-}\pi^*)$ state followed by radiationless decay via intersystem crossing (ISC) to the triplet manifold. To elucidate the electronic configuration ($n\text{-}\pi^*$ or $\pi\text{-}\pi^*$) of T_1 in the specific case of **8**, we computed the vertical electronic excitation energies to the lower excited states, as well as the relative energies of these states at their equilibrium geometries. The equilibrium geometries of the lower energy states of **8** were optimized by carrying out multiconfigurational self-consistent field (MCSCF) calculations of the complete active space (CAS) SCF class[17] with the d-polarized split-valence basis set 6-31G(d)[18] using analytical gradient procedures.[19] The active space consisted of six electrons and five orbitals: the four orbitals involved in the two π system (i.e., the π and π^* orbitals on the carbonyl and ethylene fragments) and the lone pair orbital (n) of the oxygen. Distribution of the corresponding six *active* electrons, four π electrons and two n electrons, among these five *active* orbitals leads to a CASSCF(6,5) wave function.

To incorporate the effect of dynamical valence-electron correlation on the relative energy ordering of the lower excited states of **8**, second-order multiconfigurational perturbation theory calculations based on the CASSCF(6,5) reference function (CASPT2)[20] were carried out. CASPT2 single point energies were calculated at the CASSCF(6,5)/6-31G(d) optimized geometries, using the Dunning correlation-consistent polarized valence double-ζ [9s4p1d/3s2p1d] basis set for carbon and oxygen, and [4s1p/2s1p] for hydrogen, designated cc-pVDZ,[21] and all valence electrons were correlated. Because the "normal" CASPT2 method, sometimes denoted CASPT2-0, is known to underestimate the energy of some open-shell, relative to closed-shell, electronic states, the CASPT2-g1 procedure with the full Hartree−Fock matrix was used in the construction of the zeroth-order Hamiltonian.[22]

The geometries of the relevant stationary points on the S_0 and T_1 potential energy surfaces (PESs) for the rearrangement **8** → **11** were optimized at the CASSCF level of theory with the 6-31G(d) basis set. The active space for the internal cyclopropane C−C bond cleavage in the S_0 and T_1 states of **8** consisted of six electrons and six orbitals: the four orbitals involved in the two π system (i.e., the π and π^* orbitals on the carbonyl and ethylene fragments) and the pair of σ and σ^* orbitals of the C−C bond being broken in the reaction. Distribution of the corresponding six *active* electrons, four π electrons and two σ electrons, among these six *active* orbitals leads to a CASSCF(6,6) wave function. The optimization of the transition structure for the 1,2-hydrogen shift in the S_0 and T_1 states of intermediate **10** requires increasing this CAS by adding the pair of σ and σ^* orbitals of the migrating C−H bond, leading to a CASSCF(8,8) wave function. To obtain comparable energies, single point CASSCF(8,8) calculations with the latter CAS were carried out for the S_0 and T_1 states of the intermediates **10** and **11** at the CASSCF(6,6)/6-31G(d) optimized geometries.

All of the stationary points were characterized by their harmonic vibrational frequencies as minima or saddle points. The harmonic vibrational frequencies were obtained by diagonalizing the mass-weighted Cartesian force constant matrix calculated analytically at the CASSCF level of theory with the 6-31G(d) basis set. The unscaled CASSCF/6-31G(d) frequencies were used to compute the zero-point vibrational energy (ZPVE) corrections to the energies. Connections of the transition structures between designated minima were confirmed by intrinsic reaction coordinate (IRC) calculations[23] at the CASSCF/6-31G(d) level.

Because the S_0 and T_1 states of **10** turn out to be essentially degenerate, spin-inversion mediated surface hopping could be expected to occur at the lowest-energy crossing point on the crossing seam of both PESs. These points were optimized using the algorithm of Bearpark et al.[24] within the formalism of the state-averaged MCSCF method at the CASSCF(6,6)/6-31G(d) level of theory. A weighting of 50%/50% was assigned to the S_0 and T_1 states in the state-averaging procedure. To estimate the probability of the intersystem crossing (ISC), the spin−orbit coupling (SOC) between the S_0 and T_1 states was calculated at the lowest-energy crossing points using a one-electron approximate spin−orbit Hamiltonian with the effective nuclear charges C 3.6 and O 5.6 optimized by Koseki et al.[25] For the SOC computations, state-averaged CASSCF(6,6) orbitals were used.

The relative energy ordering of the relevant stationary points on the S_0 and T_1 PESs was obtained from CASPT2-g1 single point energies calculated at the CASSCF/6-31G(d) optimized geometries, using the Dunning correlation-consistent polarized valence triple-ζ [10s5p2d1f/4s3p2d1f] basis set for carbon and oxygen, and [5s2p1d/3s2p1d] for hydrogen, designated cc-pVTZ,[21] and all valence electrons were correlated. Relative energies discussed in the text refer to energies computed at the CASPT2-g1/cc-pVTZ level unless stated otherwise. Our best total energies at 0 K correspond to the sum of the CASPT2-g1/cc-pVTZ energy and ZPVE correction.

The CASSCF calculations were carried out with the Gaussian 98 system of programs,[26] whereas the CASPT2 computations were performed with the MOLCAS 5 program package.[27]

Results and Discussion

Selected geometrical parameters of the structures of all intermediates and transition states calculated in the present paper for the thermal and photochemical rearrangement of **8** to give **11** are shown in Figures 1−4 (bond lengths in Å), which are computer-generated plots of the CASSCF/6-31G(d)-optimized geometries. The Cartesian coordinates of all structures reported in this paper are available as Supporting Information. Vertical electronic excitation energies of the lower excited states of **8**,

(17) For a review, see: Roos, B. O. *Adv. Chem. Phys.* **1987**, *69*, 399.
(18) Hariharan, P. C.; Pople, J. A. *Theor. Chim. Acta* **1973**, *28*, 213.
(19) (a) Schlegel, H. B. *J. Comput. Chem.* **1982**, *3*, 214. (b) Bofill, J. M. *J. Comput. Chem.* **1994**, *15*, 1.
(20) (a) Anderson, K.; Malmqvist, P.-A.; Roos, B. O.; Sadlej, A. J.; Wolinski, K. *J. Phys. Chem.* **1990**, *94*, 5483. (b) Anderson, K.; Malmqvist, P.-A.; Roos, B. O. *J. Chem. Phys.* **1992**, *96*, 1218.
(21) Dunning, T. H. *J. Chem. Phys.* **1989**, *90*, 1007.
(22) Anderson, K. *Theor. Chim. Acta* **1995**, *91*, 31.
(23) (a) Fukui, K. *Acc. Chem. Res.* **1981**, *14*, 363. (b) Schmidt, M. W.; Gordon, M. S.; Dupuis, M. *J. Am. Chem. Soc.* **1985**, *107*, 2585. (c) Gonzalez, C.; Schlegel, B. *J. Chem. Phys.* **1989**, *90*, 2154. (d) Gonzalez, C.; Schlegel, B. *J. Phys. Chem.* **1990**, *94*, 5523.
(24) (a) Ragazos, I. N.; Robb, M. A.; Bernardi, F.; Olivucci, M. *Chem. Phys. Lett.* **1992**, *197*, 217. (b) Bearpark, M. J.; Robb, M. A.; Schlegel, H. B. *Chem. Phys. Lett.* **1994**, *223*, 269.
(25) Koseki, S.; Schmidt, M. W.; Gordon, M. S. *J. Phys. Chem.* **1992**, *96*, 10768−10772.
(26) Frisch, M. J.; Trucks, G. W.; Schlegel, H. B.; Scuseria, M. A.; Robb, M. A.; Cheeseman, J. R.; Zakrzewski, V. G.; Montgomery, J. A.; Stratmann, R. E.; Burant, J. C.; Dapprich, S.; Milliam, J. M.; Daniels, A. D.; Kudin, K. N.; Strain, M. C.; Farkas, O.; Tomasi, J.; Barone, V.; Cossi, M.; Cammi, R.; Mennucci, B.; Pomelli, C.; Adamo, C.; Clifford, S.; Ochterski, J.; Petersson, G. A.; Ayala, P. Y.; Cui, Q.; Morokuma, K.; Malick, D. K.; Rabuck, A. D.; Raghavachari, K.; Foresman, J. B.; Cioslowski, J.; Ortiz, J. V.; Stefanow, B. B.; Liu, G.; Liashenko, A.; Piskorz, P.; Komaromi, A.; Gomperts, R.; Martin, R. L.; Fox, D. J.; Keith, T.; Al-Laham, M. A.; Peng, C. Y.; Nanayakkara, A.; Gonzalez, C.; Challacombe, M.; Gill, P. M. W.; Johnson, B. G.; Chen, W.; Wong, M. W.; Andres, J. L.; Head-Gordon, M.; Replogle, E. S.; Pople, J. A. *Gaussian 98*, revision A.9; Gaussian, Inc.: Pittsburgh, PA, 1998.
(27) Andersson, K., Barysz, M.; Bernhardsson, A.; Blomberg, M. R. A.; Cooper, D. L.; Fleig, T.; Fülscher, M. P.; DeGraaf, C.; Hess, B. A.; Karlström, G.; Lindh, R.; Malmqvist, P.-Å.; Neogrády, P.; Olsen, J.; Roos, B. O.; Sadlej, A. J.; Schütz, M.; Schimmelpfennig, B.; Seijo, L.; Serrano-Andrés, L.; Siegbahn, P. E. M.; Stålring, J.; Thorsteinsson, T.; Veryazov, V.; Widmark, P.-O. *MOLCAS version 5*; Lund University, Sweden, 2000.

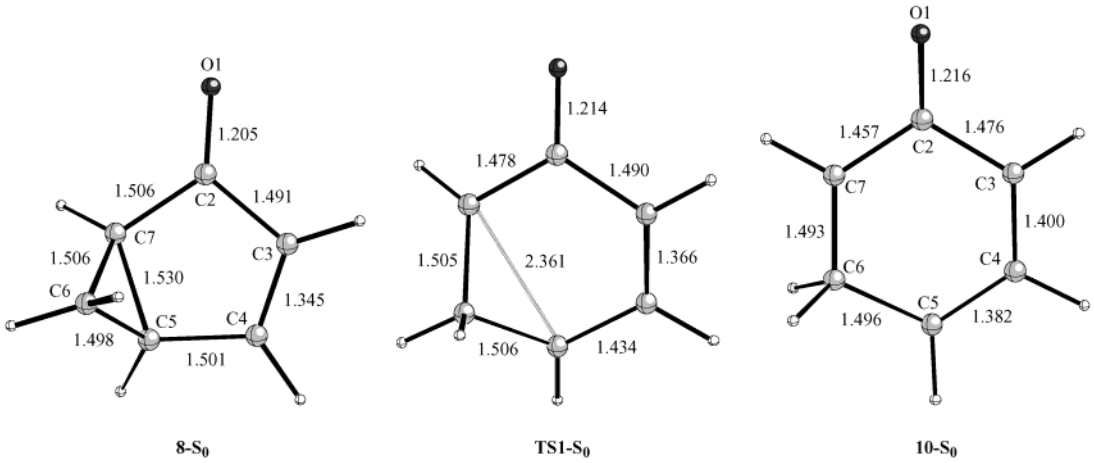

Figure 1. Selected parameters of the CASSCF/6-31G(d) optimized geometries of the stationary points on the potential energy surface of the S_0 state for the cyclopropane ring-opening **8** → **10**. Distances are given in angstroms.

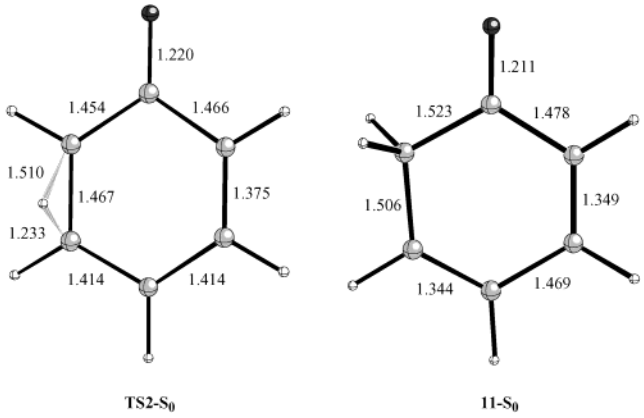

Figure 2. Selected parameters of the CASSCF/6-31G(d) optimized geometries of the stationary points on the potential energy surface of the S_0 state for the 1,2-hydrogen atom migration **10** → **11**. Distances are given in angstroms.

as well as the relative energies of these states at their equilibrium geometries, are given in Table 1. Calculated relative energies of stationary points on the PESs of the S_0 and T_1 states for the cyclopropane ring-opening **8** → **10** and for the 1,2-hydrogen shift **10** → **11** processes are collected in Tables 2 and 3, respectively. In addition, Tables 2 and 3 contain the ZPVEs computed for these stationary points. Figures 5 and 6 show schematic energy profiles for the **8** → **10** and **10** → **11** pathways found on the S_0 and T_1 states PESs.

A. Relative Energies of the Low-Lying Electronic States of 8. At the CASSCF(6,5)/cc-pVDZ level of theory, the lowest vertical excitation energy (89.9 kcal/mol) is computed for the electronic transition from the ground-state singlet (X^1A) to the π-π* triplet ($^3A(\pi$-π*)). However, the vertical excitation energy computed for the n-π* triplet (^3A(n-π*)) is only 0.7 kcal/mol higher. Moreover, at the CASPT2/cc-pVDZ level, the vertical excitation energy predicted for the ^3A(n-π*) state is 6.4 kcal/mol *lower* than that predicted for the $^3A(\pi$-π*) state. It is worth noting that the vertical excitation energy of 85.8 kcal/mol computed at the latter level of theory for the lowest excited singlet state (^1A(n-π*)) is in reasonable agreement with the absorption maximum at 350 nm (81.7 kcal/mol) observed in the UV spectra of the 3-substituted bicyclo[3.1.0]hex-3-en-2-ones **6**.[13]

Both the CASSCF(6,5)/cc-pVDZ and the CASPT2/cc-pVDZ calculations predict the $^3A(\pi$-π*) state to be the lowest excited state of **8**. This result is in accordance with many experimental findings[28] and with a recent theoretical study of triplet lifetimes of cyclic α,β-enones by Robb and co-workers.[29] In that study, the triplet π-π* state is also predicted to be the lowest-energy triplet of cyclopentenone, cyclohexenone, and cycloheptenone. Thus, it is reasonable to identify the $^3A(\pi$-π*) state of **8** as the state on whose PES the photochemical rearrangement of substituted bicyclo[3.1.0]hex-3-en-2-ones yielding substituted phenols occurs.

In this theoretical study, we have not investigated the details concerning the photophysical process leading to the formation of T_1 after initial photoexcitation from S_0 to an excited singlet state followed by radiationless decay via ISC to the triplet manifold. However, we note that the photochemistry and photophysics of the simplest α,β-enone, acrolein, have recently been studied using CASSCF calculations.[30] After photoexcitation, *s-trans*-acrolein (**12**) relaxes to a planar S_1 ^{1}(n-π*) excited-state minimum. From this point, a radiationless decay via ISC

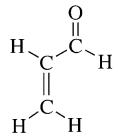

12

to the triplet manifold leads to the production of a short-lived T_1 $^3(\pi$-π*) intermediate with a twisted C=C bond (i.e., the H−C=C−H dihedral angle was calculated to be 90°). Although in cyclic enone **8** the twisting around the C=C bond is somewhat constrained due to the five-membered ring rigidity, our CASSCF(6,5)/6-31G(d) calculations predict a H−C=C−H

(28) (a) Marsh, G.; Kearns, D. R.; Schaffner, K. *J. Am. Chem. Soc.* **1971**, *93*, 3129−3137. (b) Bonneau, R. *J. Am. Chem. Soc.* **1980**, *102*, 3816−3822. (c) Schuster, D. I.; Greenberg, M. M.; Nunez, I. M.; Tucker, P. C. *J. Org. Chem.* **1983**, *48*, 2616−2619. (d) Schuster, D. I.; Heibel, G. E.; Brown, P. B.; Turro, N. J.; Kumar, C. V. *J. Am. Chem. Soc.* **1988**, *110*, 8261−8263. (e) Schuster, D. I.; Dunn, D. A.; Heibel, G. E.; Brown, P. B.; Rao, J. M.; Woning, J.; Bonneau, R. *J. Am. Chem. Soc.* **1991**, *113*, 6245−6255. (f) Dauben, W. G.; Gogen, J. M.; Ganzer, G. A.; Behar, V. *J. Am. Chem. Soc.* **1991**, *113*, 5817−5824.
(29) Garcia-Exposito, E.; Bearpark, M. J.; Ortuño, R. M.; Branchadell, V.; Robb, M. A.; Wilsey, S. *J. Org. Chem.* **2001**, *66*, 18811−8814.
(30) Reguero, M.; Olivucci, M.; Bernardi, F.; Robb, M. A. *J. Am. Chem. Soc.* **1994**, *116*, 2103−2114.

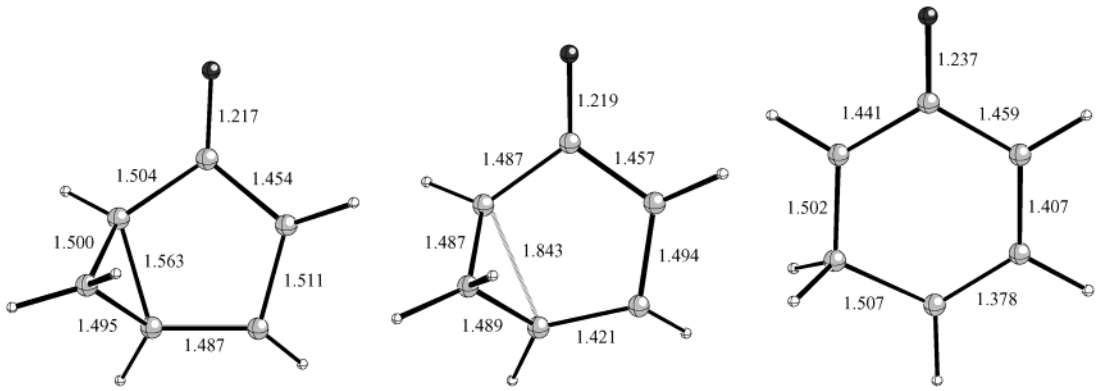

8-T_1 **TS1-T_1** **10-T_1**

Figure 3. Selected parameters of the CASSCF/6-31G(d) optimized geometries of the stationary points on the potential energy surface of the T_1 state for the cyclopropane ring-opening **8** → **10**. Distances are given in angstroms.

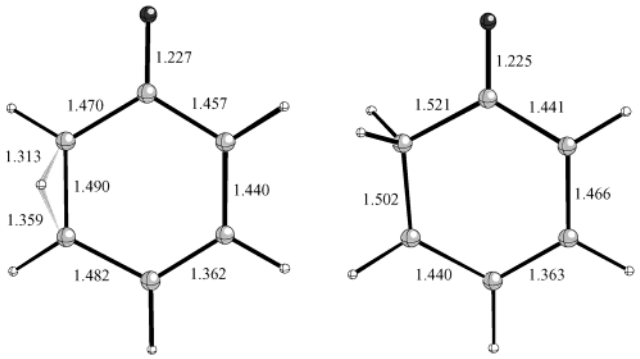

TS2-T_1 **11-T_1**

Figure 4. Selected parameters of the CASSCF/6-31G(d) optimized geometries of the stationary points on the potential energy surface of the T_1 state for the 1,2-hydrogen atom migration **10** → **11**. Distances are given in angstroms.

Table 1. Vertical Excitation Energies (VEE, kcal/mol) and Relative Energies (*E*, kcal/mol) Calculated at Different Levels of Theory with the cc-pVDZ Basis Set[a] for the Lower Excited States of **8**

	VEE		*E*	
state	CASSCF(6,5)	CASPT2	CASSCF(6,5)	CASPT2
X ^{1}A	0.0[b]	0.0[c]	0.0[b]	0.0[c]
^{3}A(π-π*)	89.9	86.3	67.0	65.9
^{3}A(n-π*)	90.6	79.9	74.2	69.8
^{1}A(n-π*)	95.7	85.8	77.1	74.1

[a] Using the CASSCF(6,5)/6-31G(d) optimized geometries. [b] Relative to −305.59647 hartrees. [c] Relative to −306.51437 hartrees.

dihedral angle of 63.1°. Therefore, it is likely that the photophysical process leading to the formation of T_1 in the case of **8** should parallel that of **12**.

B. Thermal Rearrangement of 8 To Give 11. The rearrangement of **8** to **11** on the PES of the S_0 state is predicted to occur via a two-step mechanism (see Figures 5 and 6) where the internal cyclopropane C−C bond is cleaved first leading to the formation of a singlet intermediate **10**. Subsequently, this intermediate undergoes a 1,2-hydrogen shift to give **11**. The equilibrium structures optimized for the S_0 state of **8**, **10**, and **11** are designated by **8-S_0**, **10-S_0**, and **11-S_0**, respectively, in Figures 1 and 2. The transition structures optimized for the C5−C7 bond scission in **8-S_0** and the 1,2-hydrogen shift in **10-S_0** are designated by **TS1-S_0** and **TS2-S_0**, respectively, in Figures 1 and 2.

Table 2. Relative Energies (*E*, kcal/mol) Calculated at Different Levels of Theory[a] and Zero-Point Vibrational Energies (ZPVE, kcal/mol) of Stationary Points on the Lowest Singlet and Triplet States Potential Energy Surfaces for the Cyclopropane Ring-Opening in **8**

	E			
structure[b]	CASSCF(6,6) 6-31G(d)	CASSCF(6,6) cc-pVTZ	CASPT2 cc-pVTZ	ZPVE[c]
8-S_0	0.0[d]	0.0[e]	0.0[f]	69.3
TS1-S_0	36.6	37.2	44.8	65.7
10-S_0	24.4	24.4	27.4	66.9
8-T_1	67.7	68.6	68.6	67.2
TS1-T_1	73.5	73.9	69.3	66.1
10-T_1	23.4	24.4	31.2	66.6

[a] Calculated at the CASSCF(6,6)/6-31G(d) optimized geometries. [b] See Figures 1 and 3. [c] Calculated from the unscaled CASSCF(6,6)/6-31G(d) harmonic vibrational frequencies. [d] Relative to −305.58975 hartrees. [e] Relative to −305.69388 hartrees. [f] Relative to −306.80540 hartrees.

Table 3. Relative Energies (*E*, kcal/mol) Calculated at Different Levels of Theory[a] and Zero-Point Vibrational Energies (ZPVE, kcal/mol) of Stationary Points on the Lowest Singlet and Triplet States Potential Energy Surfaces for the 1,2-Hydrogen Atom Migration in **10**

	E			
structure[b]	CASSCF(8,8) 6-31G(d)	CASSCF(8,8) cc-pVTZ	CASPT2 cc-pVTZ	ZPVE[c]
10-S_0	0.0[d]	0.0[e]	0.0[f]	66.9
TS2-S_0	18.7	15.8	4.3	65.3
11-S_0	−46.0	−46.1	−38.5	68.6
10-T_1	−1.1	−0.1	3.6	66.6
TS2-T_1	58.4	56.6	50.5	63.0
11-T_1	6.5	7.2	10.2	66.3

[a] At the CASSCF(6,6)/6-31G(d) optimized geometries of **10-S_0**, **11-S_0**, **10-T_1**, and **11-T_1** and at the CASSCF(8,8)/6-31G(d) optimized geometries of **TS2-S_0** and **TS2-T_1**. [b] See Figures 2 and 4. [c] Calculated from the unscaled CASSCF(6,6)/6-31G(d) harmonic vibrational frequencies of **10-S_0**, **11-S_0**, **10-T_1**, and **11-T_1** and the unscaled CASSCF(8,8)/6-31G(d) harmonic vibrational frequencies of **TS2-S_0** and **TS2-T_1**. [d] Relative to −305.56698 hartrees. [e] Relative to −305.67115 hartrees. [f] Relative to −306.76280 hartrees.

It is worth noting that the C5−C7 bond distance in **TS1-S_0** (2.361 Å) is close to its value (2.525 Å) in the intermediate **10-S_0**, indicating that this bond is almost completely broken at the transition structure. However, the C6−C7−C5−C4 dihedral angle in **TS1-S_0** (136.4°) is closer to its value in **8-S_0** (110.3°) than in **10-S_0** (180.0°). At 0 K, the rearrangement of **8-S_0** to **10-S_0** is predicted to be endoergic by 25.0 kcal/mol with an

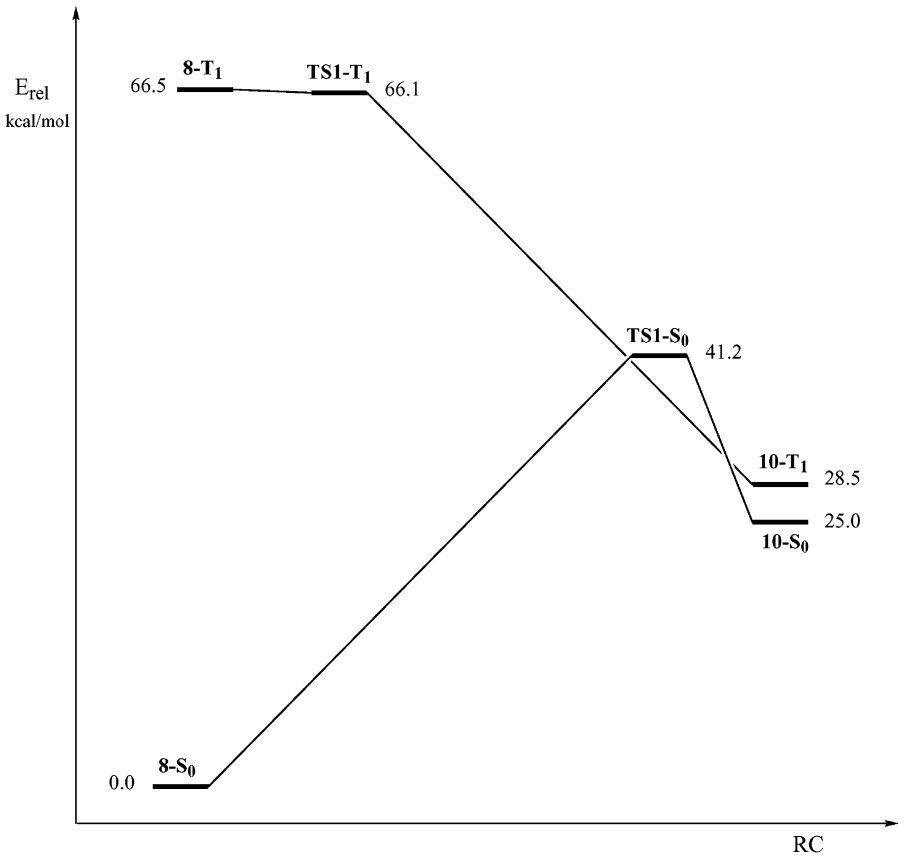

Figure 5. Schematic energy profile along an arbitrary reaction coordinate showing the structures concerning the cyclopropane ring-opening **8** → **10** on the potential energy surfaces of the S_0 and T_1 states. Energy values obtained from ZPVE-corrected CASPT2/cc-pVTZ total energies are relative to that of the S_0 state of **8**.

energy barrier of 41.2 kcal/mol (see Table 2). On the other hand, at 0 K, the 1,2-hydrogen shift in **10-S$_0$** leading to the formation of **11-S$_0$** is calculated to be exoergic by 36.8 kcal/mol, involving an energy barrier of only 2.7 kcal/mol (see Table 3). Thus, **10-S$_0$** is predicted to be a short-lived intermediate on the S_0 state PES. These results indicate that the rate-determining step of the thermal rearrangement of **8** to yield **11** is the opening of the three-membered ring in **8** leading to the intermediate **10**. The overall rearrangement is exoergic by approximately 12 kcal/mol, and the global energy barrier is calculated to be 41.2 kcal/mol at 0 K. This predicted high energy barrier is consistent with the fact that the thermal rearrangement of **1** to **2** is carried out by heating at 280 °C.

C. Photochemical Rearrangement of 8 To Give 11. We found the rearrangement of **8** to **11** on the T_1 PES also occurs via a stepwise mechanism (see Figures 5 and 6) involving the cleavage of the internal cyclopropane C−C bond leading to an intermediate **10**, which eventually may undergo a 1,2-hydrogen shift to produce **11**. The equilibrium structures optimized for the T_1 state of **8**, **10**, and **11** are designated by **8-T$_1$**, **10-T$_1$**, and **11-T$_1$**, respectively, in Figures 3 and 4. The transition structures optimized for the C5−C7 bond cleavage in **8-T$_1$** and the 1,2-hydrogen shift in **10-T$_1$** are designated by **TS1-T$_1$** and **TS2-T$_1$**, respectively, in Figures 3 and 4.

Table 2 shows that at the CASSCF/6-31G(d) level of theory, the lowest-energy triplet state of **8** (structure **8-T$_1$**) lies 67.7 kcal/mol above the energy of the ground-state singlet (structure **8-S$_0$**). This singlet−triplet energy difference is 3.4 kcal/mol lower than the value of 71.1 kcal/mol calculated at the same level of theory for the S_0-$T_1(\pi$-$\pi^*)$ energy separation in cyclopentenone.[29] At the CASPT2/cc-pVTZ level of theory, the energy separation between **8-S$_0$** and **8-T$_1$** is calculated to be 68.6 kcal/mol. Inclusion of the ZPVE correction to the latter value yields a singlet−triplet energy separation of 66.5 kcal/mol at 0 K.

A comparison between the geometries of structures **8-S$_0$** and **8-T$_1$** reveals that C2−O1 bond lengths in these structures differ by less than 0.02 Å, while the C3−C4 bond distance is notably longer (by 0.166 Å) in the structure of the triplet state. This result is consistent with the electronic feature that $\pi \rightarrow \pi^*$ excitation in T_1 is localized on the alkene moiety. It is worth mentioning that the twisting around the C3−C4 bond, measured by the C2−C3−C4−C5 dihedral angle of −14.7°, is somewhat smaller than in the case of the $^3(\pi$-$\pi^*)$ state of cyclopentenone (−23°).[29] This result can easily be rationalized from the higher rigidity of the five-membered ring of the bicyclic system **8**.

At the CASPT2/cc-pVTZ level, the rearrangement of **8-T$_1$** to **10-T$_1$** is calculated to be exoergic by 37.4 kcal/mol with an energy barrier of only 0.7 kcal/mol (see Table 2). The inclusion of the ZPVE corrections increases the exoergicity to 38.0 kcal/mol, and the energy barrier turns out to be −0.4 kcal/mol. According to these results, state T_1 of **8** should lead to the formation of the intermediate **10** without surmounting an energy barrier.

Concerning the 1,2-hydrogen shift in **10-T$_1$** leading to the formation of **11-T$_1$**, Table 3 shows that at the CASPT2/cc-pVTZ level this step is calculated to be endoergic by 6.6 kcal/mol and to involve an energy barrier of 46.9 kcal/mol. Thus, the

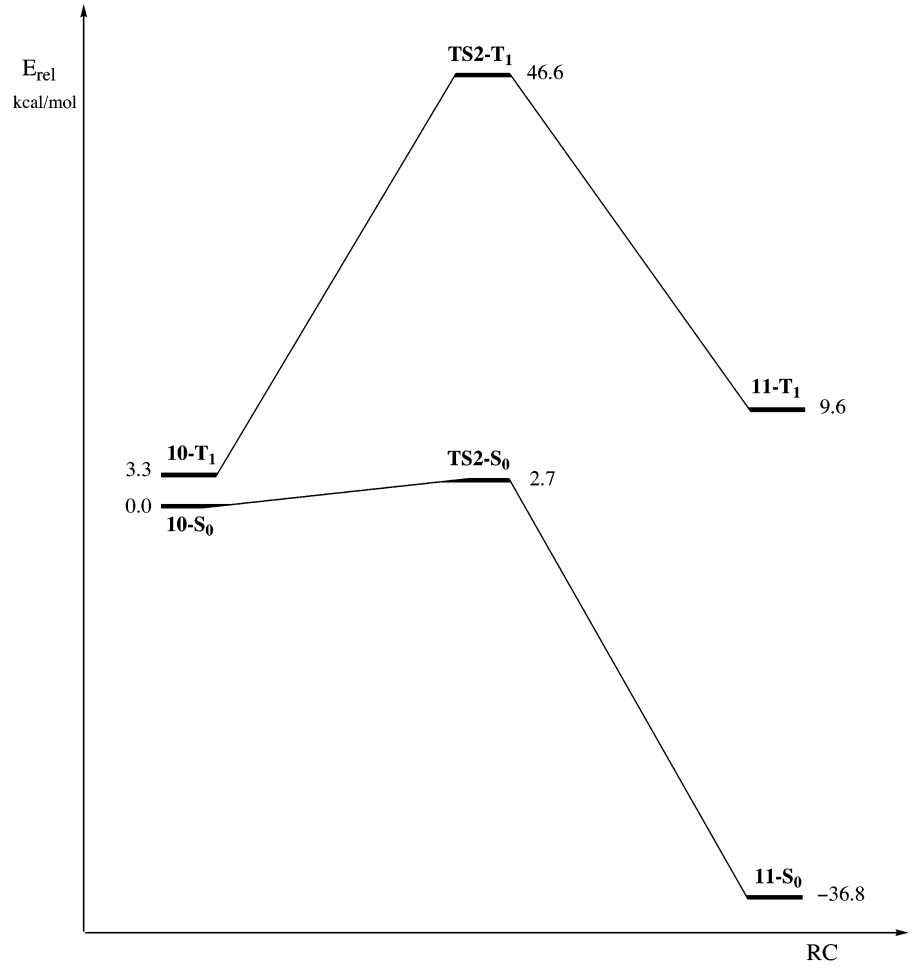

Figure 6. Schematic energy profile along an arbitrary reaction coordinate showing the structures concerning the 1,2-hydrogen atom migration **10** → **11** on the potential energy surfaces of the S_0 and T_1 states. Energy values obtained from ZPVE-corrected CASPT2/cc-pVTZ total energies are relative to that of the S_0 state of **10**.

rate-determining step for the rearrangement of **8** to **11** on the PES of the T_1 state is found to be the 1,2-hydrogen shift in the intermediate **10**. At 0 K, the global energy barrier for the **8** → **11** rearrangement on the T_1 state PES is predicted to be 43.3 kcal/mol. This energy barrier appears to be too high to be in accordance with the experimental observation that 3-substituted bicyclo[3.1.0]hex-3-en-2-ones **6** easily afford *ortho*-phenols **7** quantitatively upon sunlight exposure or irradiation at 350 nm.[14] Although when formed from **8-T1**, **10-T1** contains an excess energy of about 38 kcal/mol which is stored in vibrations and rotations, this amount of energy does not suffice for surmounting an energy barrier of about 43 kcal/mol.

As mentioned above, the 1,2-hydrogen shift **10** → **11** on the PES of the S_0 state involves an energy barrier of only 2.7 kcal/mol at 0 K. Therefore, surface hopping from the T_1 to the S_0 PES may therefore play a role. Accordingly, the T_1 state of **10** could undergo spin inversion to the S_0 state PES, followed by 1,2-hydrogen shift to **11**. The highest probability for spin inversion can be expected at the lowest-energy crossing point on the crossing seam of both PESs. Two lowest-energy crossing points, designated by **S0/T1-1** and **S0/T1-2**, were located. Selected geometrical parameters of the corresponding CASSCF/6-31G(d) optimized geometries (bond lengths in Å) are shown in Figure 7, and their relative energies are summarized in Table 4, along with the calculated SOC constants. Remarkably, at the latter level of theory, **S0/T1-1** lies 36.6 kcal/mol above the energy of

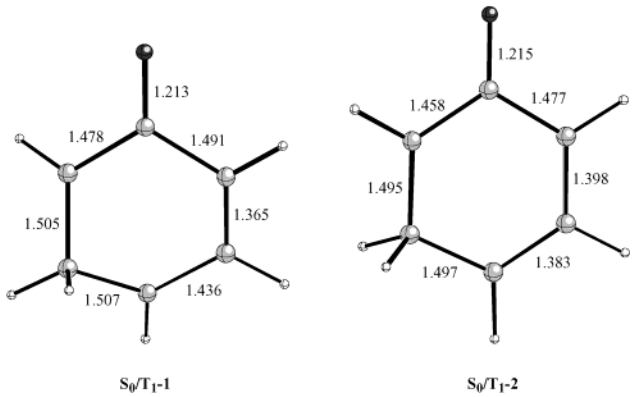

Figure 7. Selected parameters of the CASSCF/6-31G(d) optimized geometries of crossing points between the S_0 and T_1 potential energy surfaces for the cyclopropane ring-opening in **8**. Distances are given in angstroms.

8-S0, and its geometry is virtually coincident with that of the transition structure **TS1-S0**. At **S0/T1-1**, the SOC constant is calculated to be 1.2 cm^{-1}. Although small, this value may still account for an efficient spin crossing. It is interesting to note that at the **S0/T1-1** geometry, the CASPT2/cc-pVTZ calculations predict a S_0-T_1 energy difference of 2.2 kcal/mol. This is most likely due to the sensitivity of the optimum geometry of **S0/T1-1** to the inclusion of the dynamical valence-electron correlation.

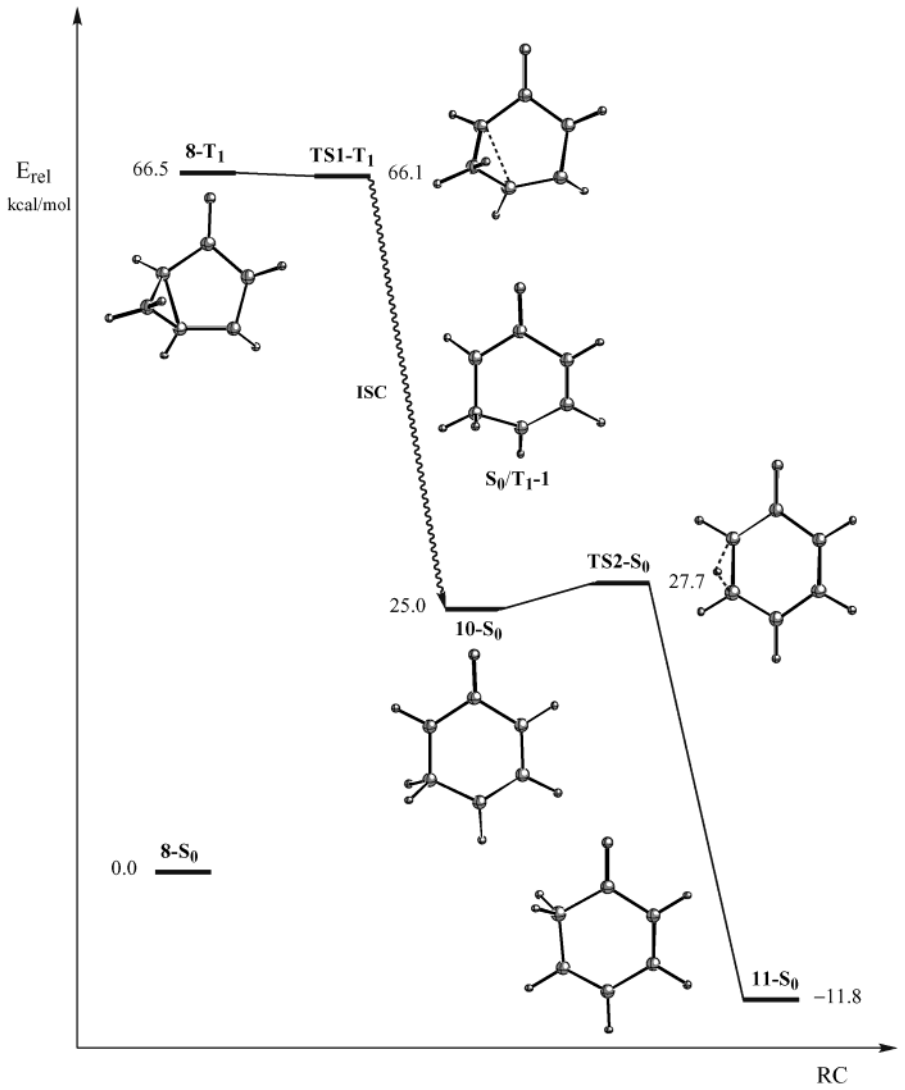

Figure 8. Schematic energy profile along an arbitrary reaction coordinate showing the structures concerning the most efficient route from **8-T_1** to **11-S_0**. Energy values obtained from ZPVE-corrected CASPT2/cc-pVTZ total energies are relative to that of the S_0 state of **8**.

Table 4. Relative Energies (*E*, kcal/mol) Calculated at Different Levels of Theory[a] and Spin−Orbit Coupling Constants[b] (SOC, cm^{-1}) of Crossing Points between the Lowest Singlet and Triplet State Potential Energy Surfaces for the Cyclopropane Ring-Opening in **8**

		E			
structure[c]	state	CASSCF(6,6) 6-31G(d)	CASSCF(6,6) cc-pVTZ	CASPT2 cc-pVTZ	SOC[d]
S_0/T_1-1	^{1}A	36.6	37.2	44.9	1.2
	A	36.7	37.4	42.7	
S_0/T_1-2	^{1}A	24.5	24.4	27.6	0.1
	A	24.5	25.2	32.7	

[a] Calculated at the CASSCF(6,6)/6-31G(d) optimized geometries. [b] Relative to the energy of **8-S_0**. [c] See Figure 5. [d] Calculated using the CASSCF(6,6)/cc-pVTZ wave function.

Regarding the crossing point **S_0/T_1-2**, at the CASSCF/6-31G(d) level of theory this structure lies 24.5 kcal/mol above the energy of **8-S_0**, and its geometry is nearly identical to that of **10-S_0**. Again we note that at the **S_0/T_1-2** geometry, the CASPT2/cc-pVTZ calculations predict a S_0-T_1 energy difference of 5.1 kcal/mol due to the effect of the dynamical valence-electron correlation on the position of the crossing point. The SOC constant calculated at **S_0/T_1-2** is extremely small (0.1 cm^{-1}), suggesting that interconversion of the S_0 and T_1 states in the region of the intermediate **10** may be inefficient. Thus, the triplet state of intermediate **10** is predicted to be experimentally accessible, because the energy barrier for isomerization to **11** via transition structure **TS1-T_1** is sufficiently large, and, furthermore, its radiationless decay to the S_0 state via ISC at the **S_0/T_1-2** crossing point is inefficient, so the triplet lifetime may suffice for its detection (e.g., by ESR spectroscopy).

On the basis of the above results, one is forced to conclude that the most efficient route from **8-T_1** to **11-S_0** is the cleavage of the internal cyclopropane C−C bond followed by radiationless decay to the S_0 state PES via ISC at the **S_0/T_1-1** crossing point, leading to the formation of the short-lived intermediate **10-S_0**, which undergoes a low barrier 1,2-hydrogen shift to give **11-S_0** via transition structure **TS2-S_0**. This route can be schematized by the reaction pathway **8-T_1** → **TS1-T_1** → **S_0/T_1-1** → **10-S_0** → **TS2-S_0** → **11-S_0** shown in Figure 8. The above-mentioned small value of the SOC constant calculated at the **S_0/T_1-1** crossing point suggests that the radiationless decay of **8-T_1** to the S_0 state PES is the rate-determining step of the photochemical rearrangement of **8** to yield **9**.

D. Electronic Nature of Intermediate 10. Regarding the electronic nature (zwitterion or diradical) of singlet intermediate **10**, it is worth noting that its optimized geometry, **10-S$_0$**, has a short C−O double bond, indicating a high degree of π-bonding. At the CASSCF/cc-pVTZ level, a dipole moment of 4.28 D and the Mulliken total charges of −0.332 and 0.252 on the carbonyl oxygen and carbon atoms, respectively, were calculated for **10-S$_0$**. These values are similar to the dipole moment of 3.48 D and the Mulliken total charges of −0.261 and 0.242 on the carbonyl oxygen and carbon atoms, calculated at the same level of theory for the bicyclic ketone **8-S$_0$**. Natural orbital analysis of the CASSCF/cc-pVTZ wave function of **10-S$_0$** further revealed this structure to be a diradicaloid singlet with frontier molecular orbital occupation numbers of 1.44 and 0.56; a "pure" diradical would have occupancies of 1.00 and 1.00. In addition, the geometry optimized for the triplet state of **10**, **10-T$_1$**, has also a short C−O double bond, indicating again a high degree of π-bonding. The unpaired electron spin density resides largely on the peripheral C3, C4, C5, and C7 carbon atoms, and the two singly occupied molecular orbitals are localized to different regions of space (i.e., one electron on the C3, C4, and C5 atoms and the other on the C7 atom). Consequently, the exchange integral between these orbitals is small, making the S_0 and T_1 states of **10** nearly identical. In fact, a comparison of the geometries of **10-S$_0$** and **10-T$_1$** reveals that these structures do not differ appreciably; the bond lengths vary at most by 0.021 Å (C2−O1 bond). Furthermore, the relative energies of Table 2 show that at the CASSCF level of theory, **10-S$_0$** and **10-T$_1$** are nearly degenerate. These geometrical and energetical findings are consistent with a diradical nature of intermediate **10**. It is worth noting that by inclusion of dynamic valence-electron correlation at the CASPT2/cc-pVTZ level, the CASSCF/cc-pVTZ singlet−triplet energy difference in **10** increases from 0.0 to 3.8 kcal/mol, singlet **10-S$_0$** being the lowest-energy state. With inclusion of the ZPVE corrections, this singlet−triplet energy gap lowers to 3.5 kcal/mol.

The computational evidence from the present study indicates the S_0 state of intermediate **10** should not be considered as a zwitterion, but rather as a diradicaloid singlet having a polarized C═O bond. This finding is in line with the results of computational studies that confirm the principally diradical (**13**) rather than zwitterionic (**14**) nature of oxyallyl systems.[31]

13 **14**

However, the finding that the intermediate derived photochemically from **8**, that **10** is best represented as a diradical (**10d**) rather than as a zwitterion (**10z**), is counter to the early mechanistic proposals.[8a,10,11] Looking carefully at the experimental data, it is worth noting that the studies of Zimmerman generating the photochemical intermediates without light[10] have been performed only in the case of **5**. In such a specific case, there is a possibility of carbocation stabilization by the aromatic rings. Moreover, from these experiments it can only be concluded that there is a common ground-state intermediate, but nothing can be said about its electronic structure. On the other hand, in the nucleophilic trapping experiments performed by Schuster,[11] there are several points to stress: First, in many of these experiments, byproducts arising from free-radical intermediates have been found. Second, the authors have found that by using alkaline salts as nucleophiles, coordination of the oxygen with the metal ion is important. Consequently, the presence of the counterion could bias the zwitterion character of the intermediate. Extensive studies to elucidate the sequence of thermal and photochemical events involved in these transformations have been performed, although, as it has been pointed out,[9] these experiments do not rule out other alternatives such as diradical intermediates. It is obvious that extension of particular experimental facts to other systems is based on the principle of analogy and must be done very carefully. Of course, a geometry optimization at the CASPT2 level of theory including the solvent effect would provide full demonstration of the diradical nature of intermediate **10**. Unfortunately, such computations are not currently possible. However, the fact that the reaction takes place neat or in noncoordinative solvents[14] clearly indicates that the solvent effect is small. Thus, it can be concluded that the present computations provide the strongest available evidence that the key intermediate **10** is a true diradical.

Conclusions

In this paper, results of CASSCF and CASPT2 ab initio calculations have been reported for equilibrium structures, transition structures, and lowest-energy crossing points on the ground state (S_0) and lowest-energy triplet state (T_1) potential energy surfaces (PESs) concerning the thermal and photochemical rearrangement of bicyclo[3.1.0]hex-3-en-2-one (**8**) to the ketonic tautomer of phenol (**11**). Analysis of these results suggest several points of potential value in understanding and interpreting the mechanism of these processes:

(1) In agreement with many experimental findings and with a recent recent CASSCF calculation of triplet lifetimes of cyclic α,β-enones, the T_1 state of **8** is predicted to be a triplet $\pi\pi^*$. At 0 K, T_1 is calculated to lie 66.5 kcal/mol above the energy of the S_0 state.

(2) On the S_0 state PES the rearrangement of **8** to **11** is predicted to occur via a two-step mechanism where the internal cyclopropane C−C bond is broken first through a high energy transition structure (**TS1-S$_0$**), leading to a singlet intermediate (**10-S$_0$**) lying 25.0 kcal/mol above the ground state of **8**. Subsequently, this intermediate undergoes a 1,2-hydrogen shift to yield **11** by surmounting an energy barrier of only 2.7 kcal/mol at 0 K. The overall reaction is exoergic by approximately 12 kcal/mol. The rate-determining step of the global rearrangement is the opening of the three-membered ring in **8**, which involves an energy barrier of 41.2 kcal/mol at 0 K. This high energy barrier is consistent with the fact that the thermal rearrangement of umbellulone (**1**) to thymol (**2**) is carried out by heating at 280 °C.

(31) (a) Osamura, Y.; Borden, W. T.; Morokuma, K. *J. Am. Chem. Soc.* **1984**, *106*, 5112−5115. (b) Ichimira, A. S.; Lathi, P. M.; Matlin, A. R. *J. Am. Chem. Soc.* **1990**, *112*, 2868−2875. (c) Powell, H. K.; Borden, W. T. *J. Org. Chem.* **1990**, *55*, 2654−2655. (d) Lim, D.; Hrovat, D. A.; Borden, W. T.; Jorgensen, W. L. *J. Am. Chem. Soc.* **1994**, *116*, 3494−3499. (e) Hrovat, D. A.; Rauk, A.; Sorensen, T. S.; Powell, H. K.; Borden, W. T. *J. Am. Chem. Soc.* **1996**, *118*, 4159−4166. (f) Matlin, A. R.; Lathi, P. M.; Appella, D.; Straumanis, A.; Lin, S.; Patel, H.; Jin, K.; Schrieber, K. P.; Pauls, J.; Raulerson, P. *J. Am. Chem. Soc.* **1999**, *121*, 2164−2173.

(3) The rearrangement of **8** to **11** on the T_1 state PES is predicted to occur via a two-step mechanism involving first an essentially barrierless cleavage of the internal cyclopropane C−C bond leading to an intermediate (**10-T_1**), which eventually may undergo a 1,2-hydrogen shift to produce **11** in its lowest-energy triplet state by surmounting an energy barrier of 43.3 kcal/mol at 0 K.

(4) Two lowest-energy crossing points between the S_0 and T_1 PESs (**S_0/T_1-1** and **S_0/T_1-2**) were located. Crossing point **S_0/T_1-1** lies about 43−45 kcal/mol above the energy of ground state **8**, and its geometry is virtually coincident with that of the transition structure **TS1-S_0**. Although the calculated SOC at this crossing point is small (1.2 cm^{-1}), it may account for a possible surface hopping from the T_1 to the S_0 PESs via ISC. On the other hand, crossing point **S_0/T_1-2** lies about 28−33 kcal/mol above the energy of ground state **8**, and its geometry is nearly identical to that of intermediate **10-S_0**. The SOC constant calculated at this crossing point is extremely small (0.1 cm^{-1}), suggesting that surface hopping from the T_1 to the S_0 PESs via ISC in this region may be inefficient. Thus, if intermediate **10-T_1** is formed, it might live long enough to be detected.

(5) The most efficient route from the T_1 state of **8** to ground state **11** is the cleavage of the internal cyclopropane C−C bond followed by radiationless decay to the S_0 state PES via ISC at the **S_0/T_1-1** crossing point, leading to the formation of **10-S_0**, which undergoes a low-barrier 1,2-hydrogen shift to give state S_0 of **11**. The small value of the SOC constant calculated at the **S_0/T_1-1** crossing point suggests that the radiationless decay from the T_1 state to the S_0 state PESs via ISC is the rate-determining step of the photochemical rearrangement of **8** to produce **11**.

(6) The structures optimized for the reaction intermediates **10-S_0** and **10-T_1** have a short C−O double bond, indicating a high degree of π-bonding. Furthermore, the two singly occupied molecular orbitals of **10-T_1** are localized to different regions of space. As a consequence, the optimum geometries of **10-S_0** and **10-T_1** do not differ appreciably, and the energy separation is predicted to be only 3.5 kcal/mol, singlet **10-S_0** being the lowest-energy state. These geometrical and energetical findings are consistent with the diradical nature of this reaction intermediate and indicate that its S_0 state should not be drawn as a zwitterion but rather as a diradical having a polarized C═O bond.

Acknowledgment. This research was supported by the Spanish DGICYT (Grants B98-1216-CO2-02 and PB98-1240-CO2-01). Additional support came from Catalonian CIRIT (Grants 2001SGR00048 and 2001SGR00315). Calculations described in this work were performed on a HP9000 J282 workstation at the University of Barcelona, a SunEnterprise 4500 at the University Rovira i Virgili, and the CPQ AlphaServer HPC320 at the Centre de Supercomputació de Catalunya (CESCA). These calculations were inspired by discussion with Dr. I. Marchueta, who did the experimental work on the photochemistry of 3-substituted bicyclo[3.1.0]hex-3-en-2-ones.

Supporting Information Available: Tables giving the Cartesian coordinates and total energies of all structures reported in this paper (PDF). This material is available free of charge via the Internet at http://pubs.acs.org.

JA0204473